Available online at www.sciencedirect.com
ScienceDirect
International Journal of Solids and Structures 45 (2008) 688–704
INTERNATIONAL JOURNAL OF SOLIDS AND STRUCTURES
www.elsevier.com/locate/ijsolstr

On irregularity-based damage detection method for cracked beams

Jialai Wang [a,*], Pizhong Qiao [b]

[a] Department of Civil, Construction, and Environmental Engineering, The University of Alabama, Tuscaloosa, AL 35487-0205, USA
[b] Department of Civil and Environmental Engineering, Washington State University, Pullman, WA 99164-2910, USA

Received 29 December 2005; received in revised form 26 August 2007
Available online 6 September 2007

Abstract

A new damage detection technique using irregularity profile of a structural mode shape is proposed in this paper. The mode-shape of a cracked beam is first obtained analytically by using a general function. Its irregularity profile is then extracted from the mode shape by a numerical filter. The location and size of the crack in the beam can be determined by the peak value appearing on the irregularity profile. Two types of numerical filters, i.e., triangular and Gaussian, are examined. It has been found that the former filter is more effective in damage detection than the latter one. Numerical simulations suggest that the irregularity-based method requires a relatively low measurement resolution. Noise stress tests are carried out to demonstrate the effectiveness and robustness of this method under the influence of noise. As a validation, the proposed method is applied to detect crack damage in an E-glass/epoxy laminated composite beam. The successful detection of the crack in the composite beam demonstrates that the irregularity-based method is capable of assessing both the location and size of the crack and can be used efficiently and effectively in damage identification and health monitoring of beam-type structures.

Keywords: Structural health monitoring; Beams; Damage detection; Irregularity; Numerical filters; Vibration; Mode shapes; Crack; Composites

1. Introduction

Structural health monitoring (SHM) is one of the most important keys in maintaining safety and integrity of the structures and avoiding loss of human life and/or monetary due to the catastrophic failure of structures. Among many SHM techniques, the dynamic response-based damage detection method (Doebling et al., 1998; Carden and Fanning, 2004) attracts most attention due to its simplicity for implementation. This technique makes use of the dynamic response of structures which offers unique information on the defects contained with these structures. Changes of physical properties of structures induced by damage

* Corresponding author. Tel.: +1 205 348 6786; fax: +1 205 348 0783.
E-mail address: JWang@eng.ua.edu (J. Wang).

0020-7683/$ - see front matter © 2007 Elsevier Ltd. All rights reserved.
doi:10.1016/j.ijsolstr.2007.08.017

can alter the dynamic responses, such as natural frequency and mode shape of the structures (Lestari et al., 2007). These parameter changes can be extracted to predict damage information, such as the presence, location and severity of damage in structures. The natural frequency provides the simplest damage detection method. Because damage tends to reduce the stiffness of the structure, a reduction of natural frequency may indicate the existence of damage in the structure. However, the natural frequency is a global feature of the structure, from which the location of the damage is difficult to be determined. To locate damage, the modal parameters (e.g., the mode shape and flexibility) are used widely, because they can capture the local perturbation induced by damage. Most recently, a general solution of the vibration of an Euler–Bernoulli beam with arbitrary type of discontinuity (e.g., crack) at arbitrary number of locations was developed by the authors Wang and Qiao (2007a), and it can be used in generic smart structures modeling and structural health monitoring of beam-type structures.

A lot of damage detection algorithms (Doebling et al., 1998; Carden and Fanning, 2004) have been developed, and they are capable of locating and sizing the damage. Most of them require the data of the health structures which are difficult to obtain and sometime unavailable. To address this issue, a few damage detection techniques which do not require the priori knowledge of healthy structures have been developed. Among them, the spatial wavelet transform method (Wang and Deng, 1999; Quek et al., 2001; Douka et al., 2003) is the most popular one. In this method, the wavelet transform is performed on the static displacement or dynamic mode shape of a cracked beam to obtain the spatially distributed wavelet coefficients. A sudden change of wavelet coefficient indicates a strong local perturbation induced by damage, and it is thus used to locate the crack. To achieve the best result of damage detection, proper mother wavelet and scale must be chosen. Numerical simulation (Quek et al., 2001) showed that it is difficult to determine the size of a vertical crack in the beam by merely examining the wavelet coefficients. To address this issue, Douka et al. (2003) proposed to use an intensity factor as an indicator of the size of the vertical crack. However, considerable extra computational effort is required. The gapped-smoothing method proposed by Ratcliffe and Bagaria (1998) is another efficient damage detection algorithm without knowing the data of undamaged structure. This method fits a gapped cubic polynomial to the modal curvature shape. The square of the difference between the curvature and the gapped cubic is defined as damage index which is then used to determine the location and size of the damage. Compared to the wavelet transform, this method has a simpler calculation scheme, but exhibiting lower accuracy in determining the location of damage. In a recent study by Hadjileontiadis et al. (2005), a novel damage detection algorithm using fractal dimension (FD) was presented. This method calculated the fractal dimension of a mode shape using a moving window. Damage location and size were determined by a peak on the FD curve indicating the local irregularity of mode shape introduced by the damage. This method successfully detected the location and size of the crack in a cantilever beam when the first mode shape was used. If the higher mode shapes were considered, this method might give misleading information as demonstrated in their study. To overcome this shortcoming, a modified FD method was recently proposed by the authors Wang and Qiao (2007b). The modified FD bears no physical meaning of the conventional FD, and therefore, it is referred to as generalized fractal dimension (GFD) (Wang and Qiao, 2007b). Three different types of damage in laminated composite beams have been successfully detected by GFD (Wang and Qiao, 2007b; Qiao et al., 2007a). However, a scale factor S has to be carefully chosen in order to detect damage successfully.

In all the above methods, the spatially distributed displacement or curvature mode shape of a beam is used, and damage is detected through looking into the local irregularity induced by the damage. In such a process, the mode shape is analogously treated as a profile of a curve. The change induced by damage becomes the irregularity of this curve. Hence, damage can be detected by directly examining the irregularity of the curve. To this end, a novel irregularity-based damage detection technique was recently proposed by Wang (2006). As a further effort, this paper tackles some fundamental application issues of this new technique which have not been addressed in the previous work (Wang, 2006).

2. Simulation of damaged beams

In this section, the analytical solutions of the free vibration of cantilever beams with single and multiple cracks are presented.

2.1. Free vibration of cracked cantilever beams

The free vibration of a cantilever beam of length L with a transverse edge crack at x_0 as shown in Fig. 1(a) is first considered. The edge crack introduces the local flexibility at the crack location, and is conventionally modeled as a rotational spring with infinitesimal thickness at the crack location (see Fig. 1(b)) (Paipetis and Dimarogonas, 1986). The rotational stiffness of the spring is determined by the fracture mechanics principle and given as (Paipetis and Dimarogonas, 1986):

$$K_T = \frac{1}{c} = 5.346\frac{h}{EI}f(a/h) \tag{1}$$

where h and a are the thickness of the beam and the depth of the crack, respectively; E and I are the modulus of elasticity and the moment inertia of the beam, respectively; $f(a/h)$ is a non-dimensional parameter determined by the crack geometry (Paipetis and Dimarogonas, 1986).

The equation of motion of the free vibration of the cracked beam shown in Fig. 1 is:

$$EIw_1''''(x,t) + \rho A\ddot{w}_1(x,t) = 0 \tag{2}$$

$$EIw_2''''(x,t) + \rho A\ddot{w}_2(x,t) = 0 \tag{3}$$

where $w_1(x,t)$ and $w_2(x,t)$ are the transverse deflections of the beams I and II, respectively; the prime and dot over $w_i (i = 1, 2)$ are the derivatives of the transverse deflection with respect to x and t, respectively; ρ and A are the density and cross section area of the beam, respectively. Denoting $\Delta w(x,t) = w_2(x,t) - w_1(x,t)$, we can express the deflection of the cracked beam in term of a general function $w(x,t)$ as:

$$w(x,t) = w_1(x,t) + \Delta w(x,t)H(x - x_0) \tag{4}$$

where $w(x,t)$ is a generalized function with discontinuity at the crack location x_0. $H(x - x_0)$ is Heaveside function which jumps from zero to unit at location x_0. Differentiating both sides of Eq. (4) with respect to x four times, we have:

$$w''''(x,t) = w_1''''(x,t) + \Delta w''''(x,t)H(x - x_0) + \Delta w'(x_0,t)\delta''(x - x_0) \tag{5}$$

where $\delta(x - x_0)$ is Dirac delta function. Combining Eqs. (2) and (3) with Eq. (5) leads to:

$$w_1''''(x,t) + \frac{\rho A}{EI}\ddot{w}_1(x,t) + \left(w_2''''(x,t) + \frac{\rho A}{EI}\ddot{w}_2(x,t) - \left(w_1''''(x,t) + \frac{\rho A}{EI}\ddot{w}_1(x,t)\right)\right)H(x - x_0) = 0 \tag{6}$$

Rearranging the above equation gives:

$$w_1''''(x,t) + \Delta w''''(x,t)H(x - x_0) = -\frac{\rho A}{EI}(\ddot{w}_1(x,t) + \Delta\ddot{w}(x,t)H(x - x_0)) \tag{7}$$

Substituting Eq. (7) into Eq. (5) yields the equation of motion of the total cracked beam:

$$w''''(x,t) + \frac{\rho A}{EI}\ddot{w}(x,t) = \Delta w'(x_0,t)\delta''(x - x_0) \tag{8}$$

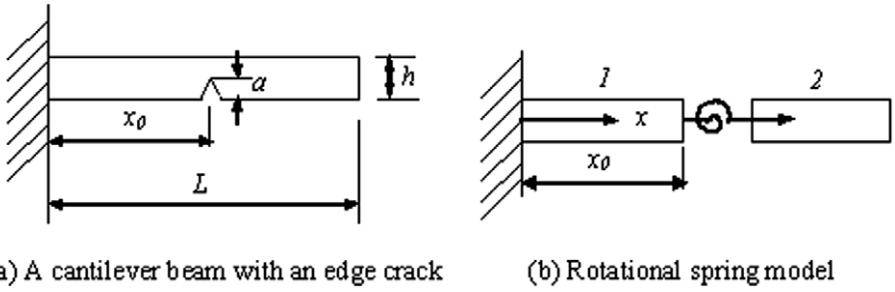

(a) A cantilever beam with an edge crack (b) Rotational spring model

Fig. 1. Cracked cantilever beam model.

Eq. (8) can be solved by the variable separation method. Let

$$w(x,t) = W(x)e^{j\omega t} \tag{9}$$

Substituting Eq. (9) into Eq. (8) yields

$$W''''(x) - \frac{\rho A\omega^2}{EI}W(x) = \Delta W'(x_0)\delta''(x-x_0) \tag{10}$$

Applying Laplace transform to both sides of Eq. (10), we have:

$$W(s) = \frac{s^3}{s^4-\lambda^4}W(0) + \frac{s^2}{s^4-\lambda^4}W'(0) + \frac{s}{s^4-\lambda^4}W''(0) + \frac{1}{s^4-\lambda^4}W'''(0) + \frac{s^2e^{-sx_0}}{s^4-\lambda^4}\Delta W'(x_0) \tag{11}$$

where $\lambda = \sqrt[4]{\frac{\rho A\omega^2}{EI}}$.

Considering the boundary conditions at the clamped end given by $W(0) = 0$ and $W'(0) = 0$, the solution of Eq. (10) can be obtained by applying inverse Laplace transform to Eq. (11) as:

$$W(x) = \frac{W''(0)}{\lambda^2}S_2(\lambda x) + \frac{W'''(0)}{\lambda^3}S_3(\lambda x) + \frac{\Delta W'(x_0)}{\lambda}S_1(\lambda(x-x_0))H(x-x_0) \tag{12}$$

where,

$$S_1(\lambda x) = \sinh(\lambda x) + \sin(\lambda x); \quad S_2(\lambda x) = \cosh(\lambda x) - \cos(\lambda x); \quad S_3(\lambda x) = \sinh(\lambda x) - \sin(\lambda x) \tag{13}$$

The boundary conditions at the free end read

$$W''(L) = 0, \quad W'''(L) = 0 \tag{14}$$

The continuity conditions at the location of the crack are given by

$$W'(x_0^+) - W'(x_0^-) = \frac{EI}{K_T}W''(x_0) \tag{15}$$

Substituting Eqs. (12) and (15) into Eq. (14) yields an eigenvalue equation of λ, which can only be solved numerically.

2.2. Free vibration of multi-cracked beams

Free vibration of a cantilever beam with multiple cracks can be solved by a similar approach as demonstrated in the above section. Consider a cantilever beam with n cracks dividing the beam into $n+1$ segments connected together through n rotational springs at the locations of the cracks in sequence. By using general function, the deflection of the cracked beam can be written as:

$$w(x,t) = w_1(x,t) + \sum_{i=1}^{n}(w_{i+1}(x,t) - w_i(x,t))H(x-x_i) \tag{16}$$

where $w_i(x,t)$ is the deflection of the i-th segment of the beam; x_i is the location of the i-th crack. Following the similar procedure in the above section, the equation of motion of the multi-cracked beam is obtained as:

$$w''''(x,t) + \frac{\rho A}{EI}\ddot{w}(x,t) = \sum_{i=1}^{n}\left(w'_{i+1}(x_i,t) - w'_i(x_i,t)\right)\delta''(x-x_i) \tag{17}$$

By using Eq. (9), the characteristic equation of mode shape reads:

$$W''''(x) - \frac{\rho A\omega^2}{EI}W(x) = \sum_{i=1}^{n}(W'(x_i+) - W'(x_i-))\delta''(x-x_i) \tag{18}$$

Following the same approach described in the above section, we have:

$$W(x) = \frac{W''(0)}{\lambda^2}S_2(\lambda x) + \frac{W'''(0)}{\lambda^3}S_3(\lambda x) + \sum_{i=1}^{n}\frac{W'_1(x_i+) - W'(x_i-)}{\lambda}S_1(\lambda(x-x_i))H(x-x_i) \tag{19}$$

where

$$W'(x_i+) - W'(x_i-) = \frac{EI}{K_{Ti}} W''(x_i) \tag{20}$$

and K_{Ti} is the stiffness of the rotational spring at location x_i and given by Eq. (1).

By using the boundary conditions at the free end (Eq. (14)), an eigenvalue problem can be established, from which the natural frequency and mode shape of the cantilever beam with n-cracks can be obtained. Noting that only two boundary conditions are used, the resultant eigenvalue problem is significantly simpler compared to the one obtained through a conventional way. The more detail of solution and application for vibration of beams with arbitrary discontinuities and boundary conditions is presented in Wang and Qiao (2007a).

3. Damage detection using irregularity

Most existing model-based damage detection methods require the baseline data of healthy structures. The damage index is usually calculated using the difference between the damaged and intact structural model data. To avoid the extra and difficult task of obtaining the data of baseline or healthy structures, a new damage detection algorithm called "irregularity-based damage detection method" was recently proposed by Wang (2006). This method is capable of detecting the damage without the knowledge of the intact structures. Some fundamental application details of this novel technique are presented in this section.

3.1. Extracting irregularity from mode shape

Consider a measured mode shape of a damaged beam shown by the solid line in Fig. 2(a). It consists of two parts: (1) the smooth part (Fig. 2(b)) showing the mode shape of the structure without damage and measurement noise, and (2) the non-smooth part (Fig. 2(c)) showing the irregularities induced by the damage in the structure and measurement noise. Only the latter part contains the information of damage. This irregular part in Fig. 2(c), however, is generally overshadowed by the smooth part of the mode shape because the signal prompting the smooth part is much stronger, as demonstrated in

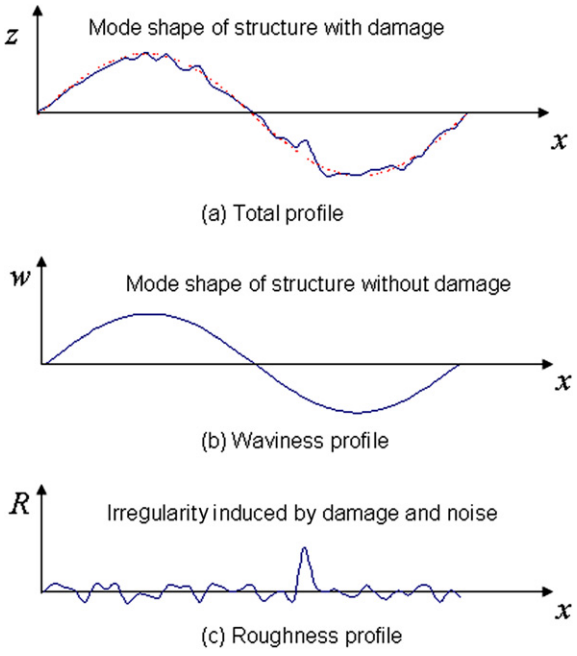

Fig. 2. Extracting irregularity from total mode shape.

Fig. 2(a). It is thus difficult to detect damage by merely examining the mode shape. To overcome this difficulty, we can extract the irregular part from the whole mode shape. Without the influence of the smooth part of the mode shape, the irregularity induced by damage can be magnified significantly as shown in Fig. 2(c). Thus, the damage can be detected easily by visual examining the irregular part of the mode shape (Fig. 2(c)). Bearing in mind the analogy between the mode shape and profile of a curve, the damage (Fig. 2(c)) can be easily extracted as the irregularity of the curve (the mode shape, Fig. 2(a)). To this end, a filter is used to eliminate the global effect (the smooth part of the mode shape (Fig. 2(b)) from the measured mode shape. Consequently, only the irregularities indicating local features of the mode shape are left and magnified on the irregularity profile. The irregularity profile (R) of a given mode shape is thus defined as

$$w(x_0) = \int_{-\infty}^{\infty} z(x_0 + x)h(x)\,\mathrm{d}x \tag{21}$$

$$R(x_0) = z(x_0) - w(x_0) \tag{22}$$

where z is the height of the mode shape; $h(x)$ is the weighted function used to smooth the mode shape. Eq. (21) is used to calculate the smooth part of the mode shape, and the resulting w is referred to as waviness of the curve (the mode shape) (Fig. 2(b)). Thus, the irregularity part (R) of the mode shape is obtained by subtracting the smooth part from the total model shape, as expressed by Eq. (22).

There are many filters available in the literature (ASME B46.1-1995, 1996; Raju et al., 2002). The most widely used one is Gaussian filter. This filter uses the following weighted function:

$$h(x) = \frac{1}{\alpha\lambda_c}\exp\left(-\pi\left(\frac{x}{\alpha\lambda_c}\right)^2\right) \tag{23}$$

where $\alpha = \sqrt{\frac{\ln 2}{\pi}}$, and λ_c is the cutoff wave-length. Triangular filter is another frequently-used one with weighted function given by:

$$h(x) = \frac{1}{B} - \left(\frac{1}{B}\right)^2 |x| \tag{24}$$

where B is the cut-off length of the filter. Compared with Gaussian filter, the triangular filter is much simpler.

3.2. Determination of crack location using irregularity profile

Numerical simulation is conducted in this section to demonstrate the feasibility of detecting damage in beams using the irregularity profiles of their vibration mode shapes. A steel cantilever beam with a length of $L = 500$ mm and thickness $h = 5.0$ mm is considered in the following simulations (Fig. 1(a)). To simulate the damage, a crack with relative depth $a/h = 0.10$ is introduced at a distance x_0 from the clamped end of the beam. In the following calculations, the resolution of mode shape is chosen as 301 uniformly distributed points along the whole beam, and the triangular filter (Eq. (24)) is employed with $B = 6.67$ mm, if not specified. By using the dynamic model established before, the first three mode shapes of the damaged beam can be obtained. A typical example of these mode shapes are presented in Fig. 3(a) for a crack locating at $x_0 = 0.3L$. It is not surprising to observe that there is no visually distinguishable irregularity on these mode shapes. Fig. 3(a) clearly shows that the crack is undetectable merely based on the mode shapes. To detect the damage, the irregularity profiles of mode shapes are obtained as shown in Fig. 3(b)–(d). The irregularity profiles of the first three respective mode shapes are obtained by Eqs. (21) and (22). Three different crack locations, i.e., $x_0 = 0.1L$, $0.4L$, and $0.7L$, are considered in Fig. 3. Note that only the absolute value of R matters when representing the severity of damage. To avoid the inconvenience in handling the sign of R, R^2 is used to construct the irregularity profiles (see Fig. 3(b)–(d) for the first three respective mode shapes), instead of the irregularity (R) itself.

In all these cases, a peak appears on the irregularity profile at the location of the crack, and it clearly indicates the existence and location of the crack. Fig. 3(b)–(d) suggest that the crack can be detected and located by the irregularity profile of the displacement mode shape.

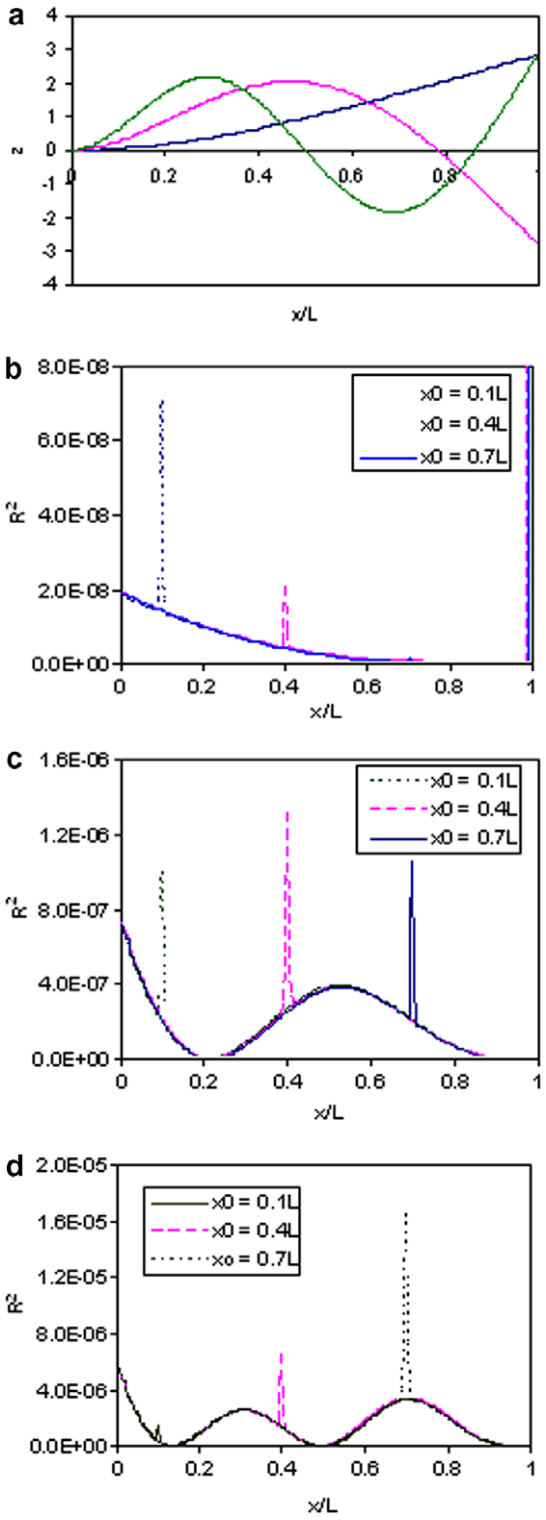

Fig. 3. Crack detection using irregularity profiles of first three mode shapes: (a) first three mode shapes of the cantilever beam with a crack at $x_0 = 0.3L$; (b) irregularity profile of the first mode shape; (c) irregularity profile of the second mode shape; (d) irregularity profile of the third mode shape.

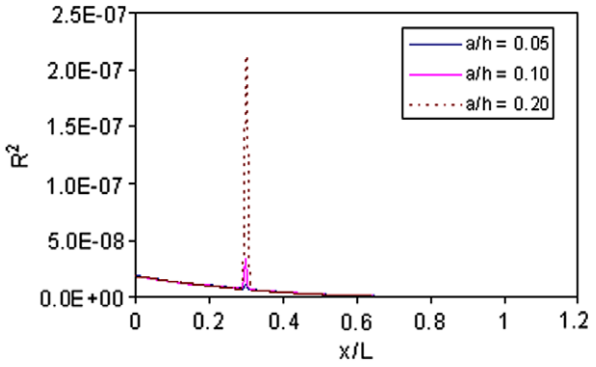

Fig. 4. Irregularity profiles of the first mode shape for three different crack depths.

3.3. Determination of crack size

The peak R^2 value at the location of the crack can be used to indicate the relative magnitude of the local irregularity induced by the crack. The trend of peak R^2 value varies with the crack size is revealed by Fig. 4. In this figure, the R^2 profiles of the previously studied cantilever beam (Fig. 1(a)) with a crack at $0.3L$ are obtained for three different crack depths, i.e., $0.05h$, $0.1h$ and $0.20h$. It can be seen that all the three irregularity (R^2) profiles are almost identical except that the peak R^2 values are different at the location of the crack. It is easy to find that the larger the crack size, the higher the peak R^2 value. This suggests that the peak R^2 value is viable of acting as an index of the relative crack size.

As demonstrated in Fig. 3(b)–(d), different peak R^2 values can be induced by cracks with the same size but at different locations. Therefore, the location of the crack must be considered in determining the size of the crack if the peak R^2 value is used. Calculations show that the peak R^2 value reduces with respect to the distance from the location of the crack to the clamped end of the beam. This is because the local perturbation induced by damage is also affected by the local bending moment, which is proportional to the second derivative of the displacement mode shape (i.e., the curvature). If the local bending moment happens to be zero, the peak R^2 value at that location is zero too. Thus a "zero location" is introduced to the peak R^2 curve (the free end for the first mode shape). If damage coincidently exists at the zero location, damage is then undetectable by the current method because the peak R^2 is zero regardless of its size. Bearing in mind that different mode shapes have different zero locations, a crack at a zero location for one mode can usually be detected by the irregularity profiles of other mode shapes.

3.4. Multiple cracks detection

In this section, a cantilever beam with two cracks at a distance of $0.3L$ and $0.5L$ from the clamped end, respectively, is examined. The relative depths (sizes) of these two cracks are the same and chosen as $a/h = 0.1$. The irregularity profile of the first mode shape is obtained using the triangular filter, and it is presented in Fig. 5. Not surprisingly, two peaks appear at the locations of the cracks on the irregularity profile, clearly indicating the existence and locations of the cracks. This suggests that multiple cracks can also be detected by the irregularity profile of mode shape. Comparing the peak R^2 values for a given crack depth, no noticeable difference is found between the present two-crack case (Fig. 5) and the single crack case (Fig. 4). This suggests that the peak R^2 value can also be used to determine the size of cracks in multi-cracked beams.

3.5. Filter effect

Although the triangular filter is used in the above calculations, other filters can also be used to calculate the irregularity profile. In Fig. 6(a), the irregularity profile of the first mode shape of a cracked beam (Fig. 1(a)) is

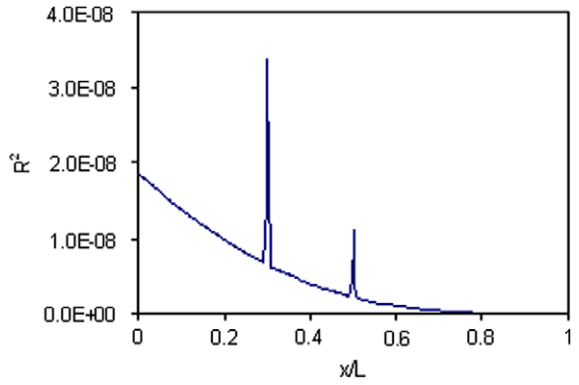

Fig. 5. Irregularity profile of the first mode shape of a beam with two cracks.

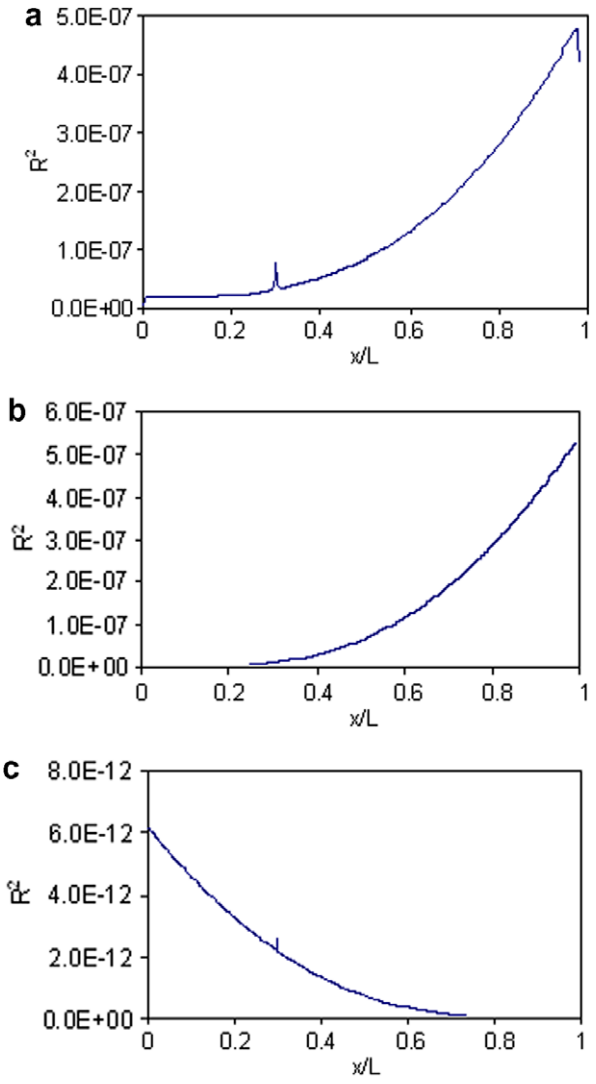

Fig. 6. Damage detection using different filters: (a) irregularity profile of the first mode shape using Gaussian filter, $a/h = 0.05$; (b) irregularity profile of the first mode shape using Gaussian filter, $a/h = 0.01$, resolution = 1000; (c) irregularity profile of the first mode shape using triangular filter, $a/h = 0.01$, resolution = 1000.

obtained using Gaussian filter (Eq. (23)) with $\alpha\lambda_c = 6.67$ mm. In this case, the crack is located at $0.3L$ from the clamped end with a relative depth of $a/h = 0.05$. A sharp peak appears on the irregularity profile at the location of the crack, indicating that the location of the damage can be successfully determined by Gaussian filter as well. In Fig. 6(b), Gaussian filter is used to detect a very small crack $a/h = 0.01$ at $0.3L$. Although a very higher resolution (1000) and very short cut-off length $\alpha\lambda_c = 2$ mm, are used, there is no distinguishable peak appearing on the irregularity profile (Fig. 6(b)). Nevertheless, if a triangular filter with $B = 2$ mm is used, the irregularity profile of the first mode shape clearly shows a peak at the location of the crack (Fig. 6(c)). Comparison of Fig. 6(b) and (c) suggests that the triangular filter is not only much simpler in calculation, but also more sensitive to damage compared with Gaussian filter. Therefore, the triangular filter is more suitable than Gaussian filter for the sake of damage detection of cracked beams.

Eq. (24) shows that B is the only parameter used in the triangular weighted function. To achieve the best damage detection result, a proper B value should be chosen. To this end, the effect of B value on damage detection is examined. Consider a cantilever beam with a crack at $x_0 = 0.4L$. The relative depth of the crack is $a/h = 0.05$. Three different B values, i.e., 3.33, 13.33, and 26.66 mm, are used to construct the irregularity profile of the first mode shape. As shown in Fig. 7, the smaller the B value, the more distinct the peak R^2 is on the

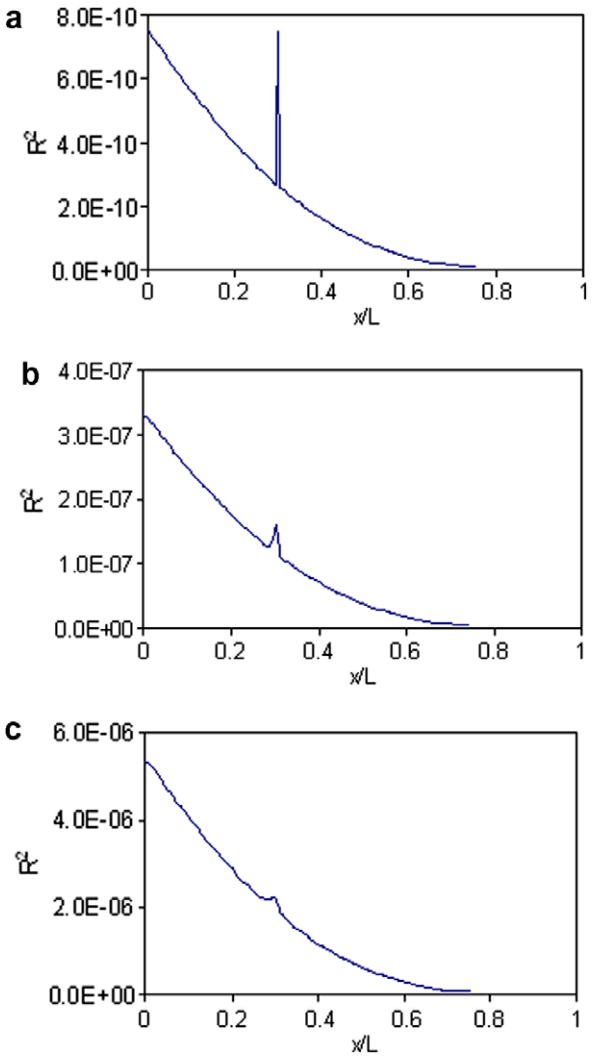

Fig. 7. Irregularity profile of the first mode shape with crack at $x_0 = 0.3L$ and crack depth of $a/h = 0.05$: (a) $B = 3.33$ mm; (b) $B = 13.33$ mm; (c) $B = 26.67$ mm.

irregularity profile. This is because B defines the cut-off length of the filter. With a smaller B, the local feature of the mode shape is more pronounced because any wavelength larger than B is filtered out. To increase the sensitivity of the irregularity profile to damage, a smaller B should be adopted. However, a smaller B requires higher resolution of mode shape and also increases the sensitivity to the measurement noise of the irregularity profile, as illustrated in the following sections.

3.6. Resolution requirement

The resolution requirement on the measurement of mode shape is very important for practical application of the proposed damage detection method. High resolution requirement may prohibit the practical application of the present method because of the high expense associated with the measurement of mode shape. In Fig. 8, the resolution requirement of the present damage detection method is examined. In Fig. 8(a), the irregularity profile of the cantilever beam with a crack of $a/h = 0.05$ at $x_0 = 0.4L$ is obtained using 56 uniformly distrib-

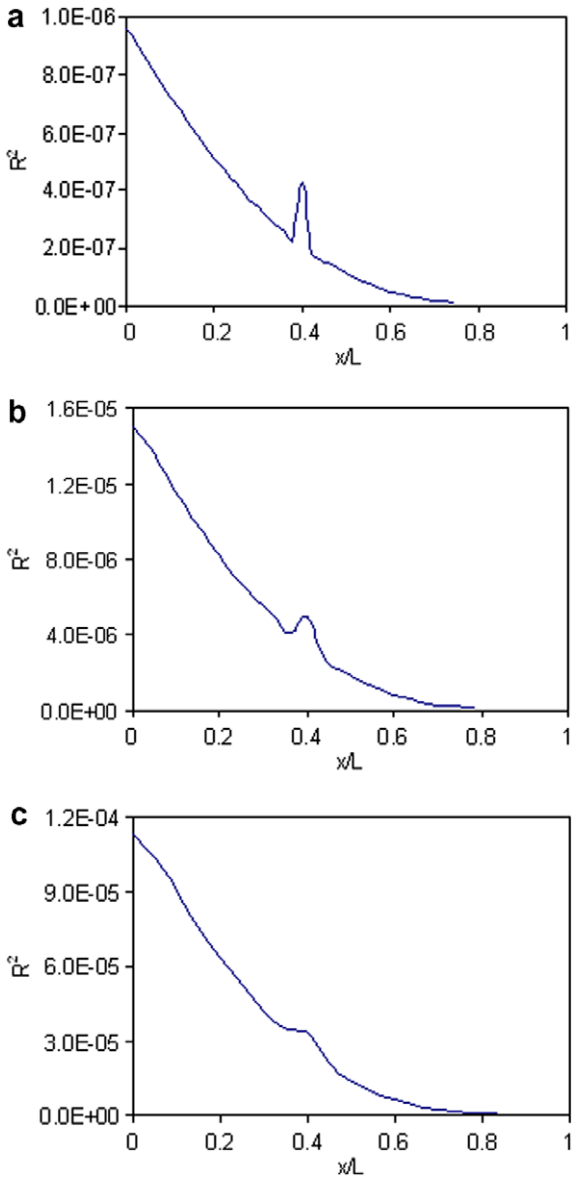

Fig. 8. Resolution effect on damage detection: (a) resolution = 56; (b) resolution = 26; (c) resolution = 16.

uted points of the first mode shape. Clearly, the damage is detectable with this resolution as shown in Fig. 8(a). Reducing the measurement points to 26, damage is still detected successfully by the irregularity profile, as shown in Fig. 8(b). Fig. 8(c) suggests that the damage can even be detected by just using 16 measurement points. Such a low resolution requirement makes the present method very viable for practical application.

3.7. Noise effect

The experimentally measured mode shape is inevitably corrupted by measurement noise and errors. The measurement noise and errors introduce local perturbations to the mode shape which can be picked up by the irregularity profile as peak values. On one hand, these peak values could be mistakenly interpreted as induced by damage and lead to false detection of damage in beams. On the other hand, they could overshadow the peak value induced by real damage in the beam and lead to missed detection of damage. Therefore, effectiveness and robustness of the present irregularity-based damage detection method under the influence of noise must be carefully examined before it can be used in real life applications confidently.

To introduce noise effect, a series of random noise is generated from a uniform distribution on the interval $[-0.5, 0.5]$ of different levels and added to the exact mode shape obtained analytically. For the convenience of calculation, the signal-to-noise ratio (SNR) at the location of the crack is used to determine the level of noise (and therefore referred as $LSNR$, following the same definition as in Hadjileontiadis et al. (2005)). In Fig. 9(a), the irregularity profile for a cantilever beam with a crack of $a/h = 0.3$ at $x_0 = 0.3L$ from the clamped end is presented with noise at $LSNR = 40$ dB. It can be seen that a lot of peak values appear on the irregularity profile due to the existence of noise. However, the most pronounced one appears at the location of the crack suggesting that damage is still detectable even with such a high level of noise. If the crack is smaller, i.e., $a/h = 0.1$, as shown in Fig. 9(b), the peak R^2 value induced by the crack becomes much smaller and indistinguishable from the others caused by the noise. In this case, damage is missed by the present method due to the presence of noise. However, if we increase the value of B from 6.67 mm used in Fig. 9(a) and (b) to 13.33 mm, the peak R^2 value induced by the real damage becomes distinguishable again at the location of the crack as shown in Fig. 9(c). As demonstrated before, a lower B value can improve the sensitivity of the irregularity to the damage. But as expense, the sensitivity of the irregularity to the measurement noise is also magnified. Therefore, a higher B value should be used to improve the robustness of the irregularity-based damage detection method under the influence of measurement noise.

The measurement noise not only affects the peak R^2 value at the location of crack, but also influences the determination of the crack size, as illustrated in Fig. 10 for a cantilevered beam with a crack at $x_0 = 0.3L$ (Fig. 1(a)). In all the subfigures of Fig. 10, 100 samples of peak R^2 values at the location of the crack are obtained for the first mode shape of the beam. The mean values of the peak R^2 values are calculated and presented by the solid lines. The upper and lower bounds of peak R^2, which are defined by the mean-value $\pm$ the standard deviation, are also presented in Fig. 10. As a reference, the corresponding peak R^2 values from the exact first mode shape with noise interference (i.e., noise-free) are also presented by a dotted line in Fig. 10. When $LSNR = 70$ dB, the mean value of peak R^2 is almost identical with the one from the exact mode shape as shown in Fig. 10(a); meanwhile, the standard deviation is very small in this case. This suggests that the effect of noise of $LSNR = 70$ dB on the determination of crack size is negligible. However, if the noise level is increased to $LSNR = 60$ dB, its effect on the crack size is much more pronounced and cannot be neglected any more as shown in Fig. 10(b). In this case, not only does the mean value of peak R^2 deviate from the exact solution, but also the standard deviation of peak R^2 values increases significantly, leading to unstable estimation of the crack size. As aforementioned, a higher B value can be used to improve the damage detection effect under the influence of the measurement noise. Fig. 10(b) is recalculated by using $B = 13.33$ mm instead of 6.67 mm, and the results are presented in Fig. 10(c). As expected, the deviation of the mean value from the exact solution and the standard deviation are reduced significantly (see Fig. 10(c)).

4. Application example

In this study, the experimental data (i.e., the curvature mode shapes) of a cantilever composite beam with a saw-cut crack obtained by Qiao et al. (2007a) are used to validate the proposed irregularity-based damage

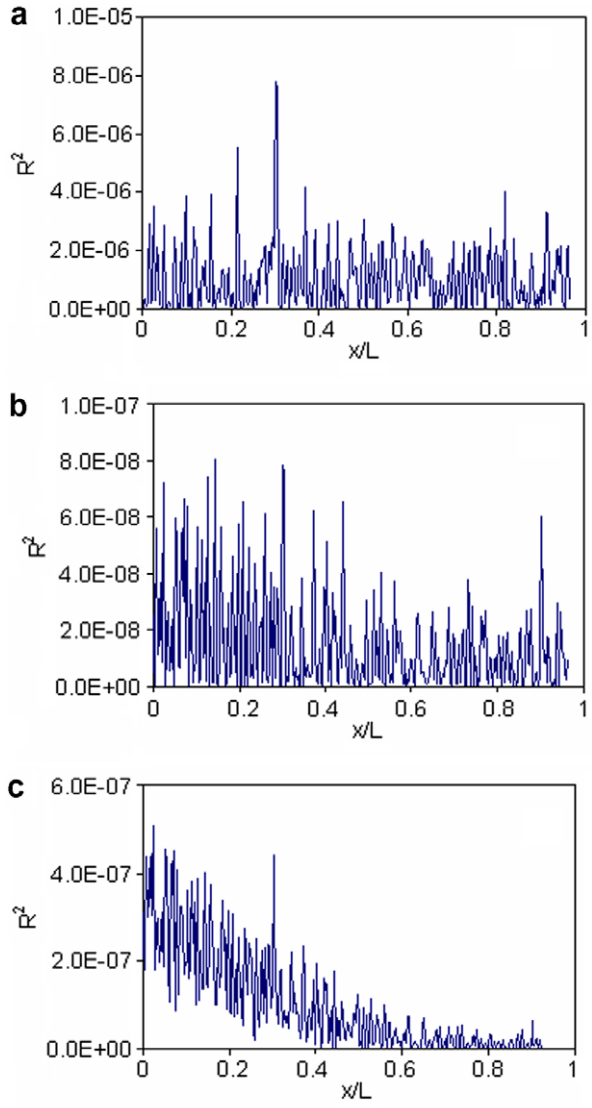

Fig. 9. Noise effect on irregularity profile: (a) $a/h = 0.3$, $LSNR = 40$ dB, $B = 6.67$ mm; (b) $a/h = 0.1$, $LSNR = 60$ dB, $B = 6.67$ mm; (c) $a/h = 0.1$, $LSNR = 60$ dB, $B = 13.33$ mm.

detection method. The tested composite beam specimens were made of E-glass fiber and epoxy resins with a $[CSM/0(90/0)_3]_S$ lay-up of total 16 layers. The size of the beam is $609.6 \times 50.8 \times 4.8$ mm. After clamped in the cantilever configuration, the free span of the specimens was 558.8 mm. A lead–zirconate–titanate (PZT) ceramic patch of 8×12 mm was attached to the specimen near the clamped end, and it acts as an actuator. The polyvinylidene fluoride (PVDF) thin polymer films of $30 \times 12 \times 28$ μm were used as sensors to obtain the curvature mode shapes. The locations of PVDF measurement points with a spacing of 25.4 mm are shown in Fig. 11. The saw-cut damage was introduced at $x_0 = 279.4$ mm (around the location of sensor 9) from the cantilevered end to simulate the crack-type damage in the composite beam. The depth of the through-width saw-cut is about half of the specimen thickness. The "curvature" mode shapes measured by the PDVF sensors are shown in Fig. 12 (due to significant noise present in the first mode shape, only the three consecutive modes from the 2nd to 4th are considered). It should be pointed out that the resulting mode shape based on the PVDF sensors is referred as "curvature" shape in Qiao et al. (2007a), which is not the actual curvature shape of the beam, rather than a linear combination of slope mode shapes of the beam (Wang and Wang, 1997).

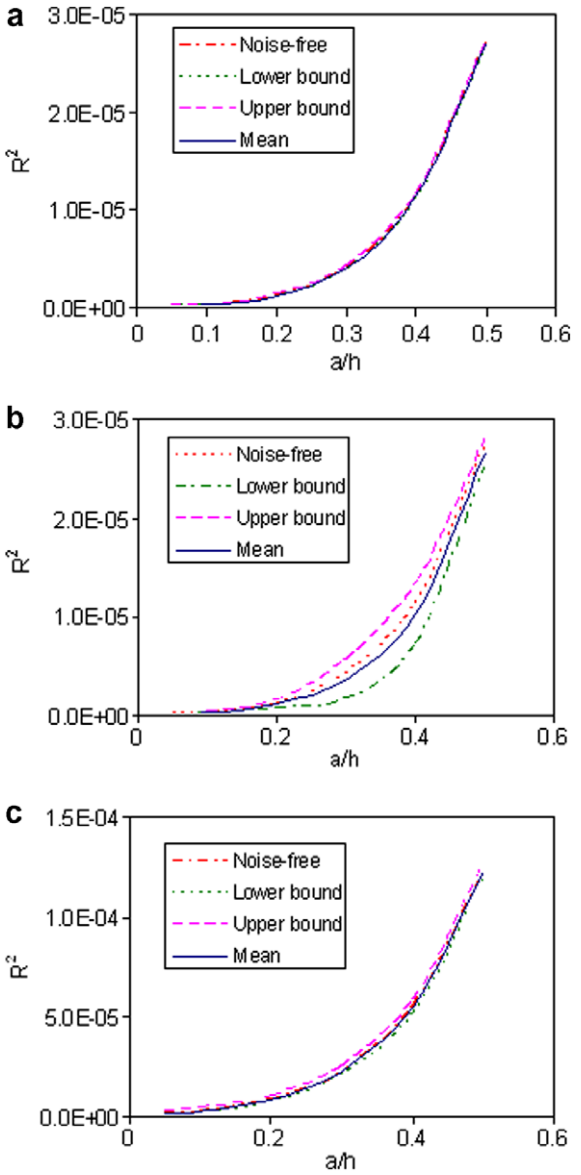

Fig. 10. Noise effect on the determination of crack size: (a) peak R^2 value varies with the size of the crack, $LSNR = 70$ dB, $B = 6.67$ mm; (b) peak R^2 value varies with the size of the crack, $LSNR = 60$ dB, $B = 6.67$ mm; (c) peak R^2 value varies with size of the crack, $LSNR = 60$ dB, $B = 13.33$ mm.

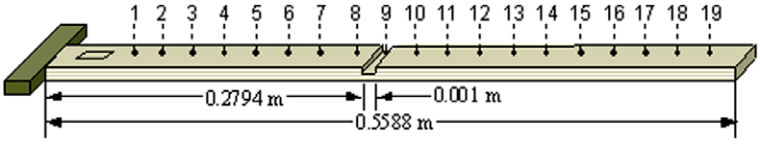

Fig. 11. Sensor layout for the composite beam with a saw-cut crack.

As demonstrated before, the slope mode shape can also be used to detect damage. By using triangular filter with B chosen as three times of the sensor spacing, the R^2 profiles of the mode shapes are obtained and presented in Fig. 13. As shown in Fig. 13, there are a few peaks appearing on the R^2 profile, of which some are

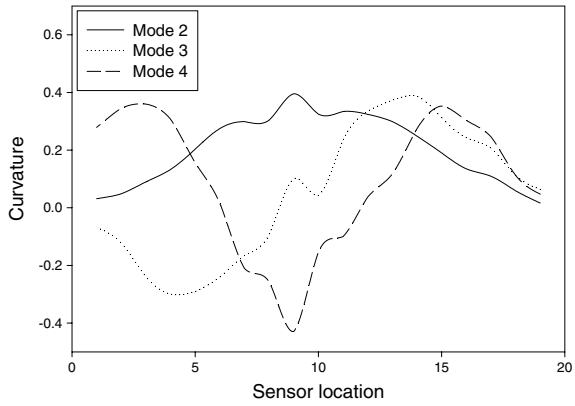

Fig. 12. "Curvature" mode shapes of saw-cut damaged beam.

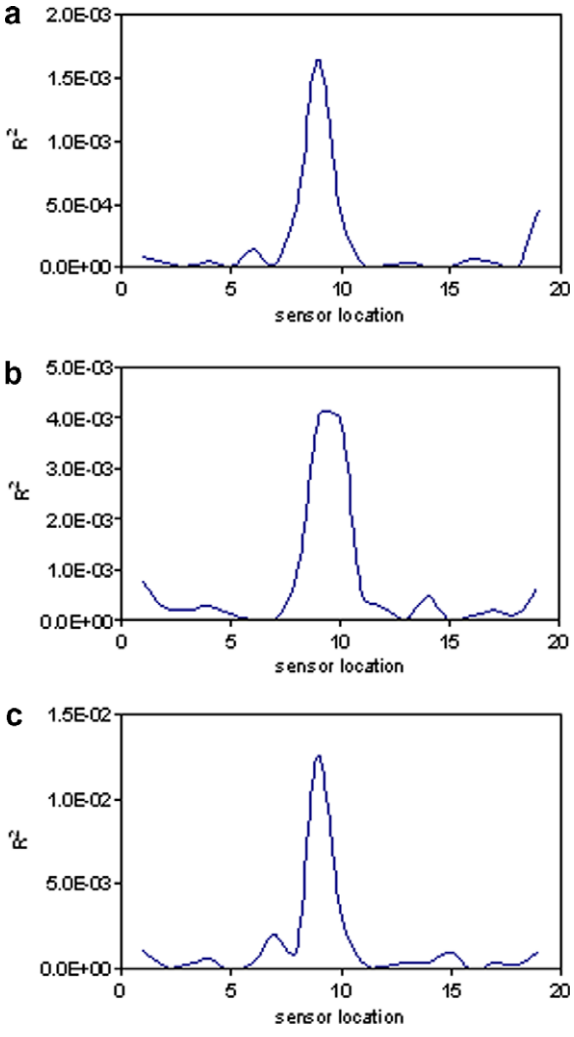

Fig. 13. R^2 profiles of the saw-cut beam: (a) mode 2; (b) mode 3; (c) mode 4.

attributed to the environmental noise or boundary conditions. As expected, the largest peak value appears at the location of the saw-cut (Sensor 9), clearly demonstrating that the proposed method can successfully detect the existence of the crack in the composite beam. Although the location of the crack could be approximated directly from the "curvature" mode shapes (Fig. 12) due to the large crack depth of the existing beam specimen (Qiao et al., 2007a), the irregularity profiles of the mode shapes exhibiting in Fig. 13 further magnify the effect of the damage at the location of crack by a much sharper peak comparing to the adjacent R^2 values.

5. Conclusions

In this paper, the fundamental issues (e.g., single crack vs. multiple cracks, crack size, Gaussian vs. triangular filters, resolution requirements, and noise effect) of irregularity-based damage detection method are addressed. It is shown that the proposed method can successfully detect not only a single crack, but also multiple cracks in beams. The location and size of a crack in beams are determined by a peak value at the location of the damage on the irregularity profile of mode shape. Compared with existing damage detection methods such as wavelet transform, the proposed method has a much easier calculation scheme and more straightforward physical meaning. For the two filters used in this study, the triangular filter demonstrates a superior potential than Gaussian filter in damage detection. The important effect of the cut-off length of the triangular filter on damage detection is also studied. It has been demonstrated that the smaller cut-off length can improve the sensitivity of the irregularity to damage; while the higher cut-off length on the other hand can enhance the robustness of the present method under the influence of noise. The potential practical application of this method is further confirmed by its low requirement on measurement resolution. The effectiveness and robustness of this method under the influence of noise has been demonstrated by the noise stress tests. The present method is then implemented on the experimentally-measured curvature mode shapes, and it successfully detects the saw-cut crack in the laminated composite beam. This method is simple to be implemented and does not require the knowledge of the healthy structure. However, it requires multiple sensors to obtain the mode shapes of structures. This is the major drawback for most of mode shape-based damage detection techniques. Nevertheless, this drawback can be overcome by more efficient and autonomous measurement techniques to obtain the mode shapes, such as scanning laser vibrometer (SLV) (Qiao et al., 2007a). The novel irregularity-based damage detection techniques examined in detail in this study can be not only used effectively and efficiently in assessing damage (in terms of location and size) in beam-type structures but also extended to two-dimensional problems such as damage detection in plates (Qiao et al., 2007b) (e.g., irregularity profile of the surface).

Acknowledgements

The first author wants to acknowledge the financial support from ND NASA EPSCoR through the NASA Grant #NCC5-582. The experimental study of this paper is based upon the work supported by the Air Force Office of Scientific Research (AFOSR) under Contract No. FA9650-04-C-0078. Any opinions, findings and conclusions, or recommendations expressed in this study are those of the authors and do not necessarily reflect the views of the AFOSR.

References

ASME B46.1-1995, 1996. Surface texture (surface roughness, waviness, and lay): an American National Standard. ASME, New York.

Carden, E.P., Fanning, P., 2004. Vibration based condition monitoring: a review. Structural Health Monitoring 3 (4), 355–377.

Doebling, S.W., Farrar, C.R., Prime, M.B., 1998. A summary review of vibration-based damage identification methods. The Shock and Vibration Digest 20, 91–105.

Douka, E., Loutridis, S., Trochidis, A., 2003. Crack identification in beams using wavelet analysis. International Journal of Solids and Structures 40, 3557–3569.

Hadjileontiadis, L.J., Douka, E., Trochidis, A., 2005. Fractal dimension analysis for crack identification in beam structures. Mechanical Systems and Signal Processing 19, 659–674.

Lestari, W., Qiao, P., Hanagud, S., 2007. Curvature mode shape-based damage assessment of carbon/epoxy composite beams. Journal of Intelligent Material Systems and Structures 18 (3), 189–208.

Paipetis, S.A., Dimarogonas, A.D., 1986. Analytical Methods in Rotor Dynamics. Elsevier Applied Science, London.
Qiao, P., Lestari, W., Shah, M., Wang, J., 2007a. Dynamics-based damage detection of laminated composite beams using contact and non-contact measurement systems. Journal of Composite Materials 41 (10), 1217–1252.
Qiao, P., Lu, K., Lestari, W., Wang, J., 2007b. Curvature mode shape-based damage detection in composite laminated plates. Composite Structures 80 (3), 409–428.
Quek, S., Wang, Q., Zhang, L., Ang, K., 2001. Sensitivity analysis of crack detection in beams by wavelet technique. International Journal of Mechanical Science 43, 2899–2910.
Raju, J., Muralikrishnan, B., Fu, S., 2002. Recent advances in separation of roughness, waviness and form. Precision Engineering 26, 222–235.
Ratcliffe, C.P., Bagaria, W.J., 1998. A vibration technique for locating delamination in a composite beam. AIAA Journal 36, 1074–1077.
Wang, B., Wang, B., 1997. Feasibility analysis of using piezoceramic transducers for cantilever beam model testing. Smart Materials and Structures 6, 106–116.
Wang, J., 2006. Damage detection in beams by roughness analysis. Sensors and Smart Structures Technologies for Civil, Mechanical, and Aerospace System, SPIE 6174-52, 26 February–2 March 2006, San Diego, CA.
Wang, J., Qiao, P., 2007a. Vibration of beams with arbitrary discontinuities and boundary conditions. Journal of Sound and Vibration 308 (1–2), 12–27.
Wang, J., Qiao, P., 2007b. Improved damage detection for beam-type structures using a uniform load surface. Structural Health Monitoring 6 (2), 99–110.
Wang, Q., Deng, X., 1999. Damage detection with spatial wavelets. International Journal of Solids and Structures 36, 927–939.